Adsorption of molecular oxygen on GaAs(001) studied using high-resolution electron energy-loss spectroscopy

E. Placidi,[1,*] C. Hogan,[2,3] F. Arciprete,[2] M. Fanfoni,[2] F. Patella,[2] R. Del Sole,[2,3] and A. Balzarotti[2]
[1]*CNR-INFM, Via della Ricerca Scientifica 1, 00133 Roma, Italy*
[2]*Dipartimento di Fisica, Università di Roma "Tor Vergata," Via della Ricerca Scientifica 1, 00133 Roma, Italy*
[3]*European Theoretical Spectroscopy Facility (ETSF) and CNR-INFM, Via della Ricerca Scientifica 1, 00133 Roma, Italy*
(Received 21 February 2006; published 24 May 2006)

High-resolution electron-energy-loss spectroscopy (EELS) has been applied to investigate the electronic structure of the GaAs(001)-$c(4\times4)$ and $\beta2(2\times4)$ reconstructions by means of successive exposure to molecular oxygen. Measurements have been performed on high-quality samples grown *in situ* by molecular beam epitaxy (MBE). We coupled the experimental findings with calculated spectra [density functional theory in the local density approximation (DFT-LDA)] to investigate the origin of surface states involved in the transitions and possible mechanisms of oxidation.

DOI: 10.1103/PhysRevB.73.205345 PACS number(s): 78.68.+m, 73.20.−r, 78.40.Fy, 79.20.Uv

I. INTRODUCTION

Exposure of a surface to gas is one of the most frequently used methods of assigning surface character to an experimental feature detected by spectroscopy. If the signal originates in the first layers of the crystal, it is reasonable to assume that it should exhibit a remarkable variation when gas adsorbs onto the surface; in fact, some surface spectroscopies have developed just by taking advantage of this idea. For example, in surface differential reflectivity[1,2] the reflection of a clean surface is compared with that of the same surface after oxidation. The influence of oxygen[3,4] and hydrogen[5] on the reflectance anisotropy spectra has also been used to separate bulk and surface related features. In some cases, much care is required for the interpretation of spectral features after gas exposure: The reaction with the gas can bring about the occurrence of new structures as observed by Arens *et al.*[6] on the GaAs(001)-$c(4\times4)$ after the exposure to the atomic hydrogen.

In recent works[7,8] we have shown how high resolution electron energy loss spectroscopy (HREELS) is a powerful tool for deducing the electronic structure of a surface, based on measurement of the *anisotropy* of the first few layers. In this work, we extend the intrinsic surface sensitivity of this approach by observing the evolution, under oxygen exposure, of the raw HREELS spectra as well as the surface anisotropy. Two surfaces of great technological importance are investigated: The As-rich (2×4) and $c(4\times4)$ reconstructions of GaAs(001). The optical and energy loss properties of both these surfaces have been extensively studied in the past. In particular, the importance of performing anisotropy measurements on the *as-grown* surface was detailed.[9,10] For the (2×4) phase, quite a lot of variation exists among published experimental reflectance anisotropy spectra, and in fact, only one recent study has succeeded in identifying true surface state features.[10] On the other hand, much of the knowledge gained over the years about the $c(4\times4)$ atomic structure has been complicated by recent revelations that the exact surface stoichiometry depends on the growth species and on kinetic factors.[11]

Much research has been carried out over the last thirty years with the aim of understanding oxide formation on GaAs, with most of the focus on the cleavage surface. For the MBE grown (001) surface, Kruse, McLean, and Kummel investigated the GaAs(001)-$c(2\times8)$ surface under oxidation using STM.[12,13] In these studies it was proposed that the two atoms of each oxygen molecule react by inserting into two neighboring As–Ga backbonds, subsequently dislodging the two As atoms from their positions. By means of detailed microscopic calculations of the energy loss spectra of the clean surfaces, we are able to reconcile the behavior of each spectral feature under oxygen exposure by considering the relevant contributing surface states, as was done for the RAS of the (2×4) surface.[4] Although fully microscopic calculations of the surface spectra of oxidized surfaces would be preferable, these are very demanding computationally, and have only been examined in a few studies.[14,15] Based on our results we suggest possible mechanisms for oxygen adsorption during the initial stages.

In the following section, we outline the experimental procedures for preparing the surfaces and obtaining the HREELS spectra. Section III contains a brief description of the computational method. Results and discussion, for the (2×4) and $c(4\times4)$ surfaces, respectively, are contained in Sec. IV and V. Conclusions are presented in the final section.

II. EXPERIMENTAL

The homoepitaxial growth of GaAs was performed on a Riber 32 MBE reactor under reflection high-energy electron diffraction (RHEED) control. n-type Si-doped ($n=1\times10^{18}$ cm^{-3}), 500 μm thick GaAs(001) wafers were mounted with In on a special Mo holder locked to the standard 3 in molyblock. The native oxide layer was removed at 630–650 °C under As flux. The substrate temperature T_s was kept at 590 °C during growth with a flux ratio $J_{As}/J_{Ga}\approx10$. After deposition of 0.5 μm of GaAs with a growth rate of 1.8 Å s^{-1}, it followed a post growth annealing for 15 min at the same temperature in As_4 flux. For the $c(4\times4)$ surface,

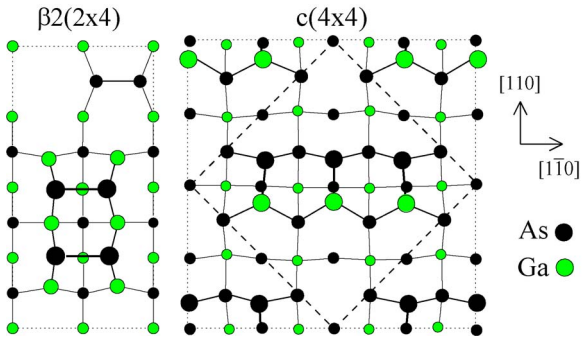

FIG. 1. (Color online) Schematic representation of the $\beta 2(2\times4)$ and $c(4\times4)$ (mixed dimer model) As-rich GaAs(001) reconstructions.

transfer outside the MBE chamber was done when the substrate temperature was about 300 °C; for the (2×4), the surface preparation was terminated with a rapid quenching, obtained by transferring the sample outside the MBE chamber immediately after switching off the sample heater. This procedure is known to give a good $\beta 2(2\times4)$ reconstruction provided the As flux is high enough to avoid the formation of As-deficient phases during quenching.

The loss spectra were taken at room temperature with fixed total angle scattering of 90° at specular reflection. The primary electron beam of 15 eV was incident on the surface at 45° with respect to the sample normal, and the acceptance angle of the electron analyzer was about 2°. In these conditions $q_{\parallel}$ reaches approximately 0.25 Å at loss energies of 5 eV.

Oxidation was performed by introducing molecular oxygen into the ultra high vacuum (UHV) preparation chamber via a leak valve. During gas exposure the sample was kept at room temperature in a pressure value around $10^{-8}-10^{-7}$ mbar. Prior to measuring a new HREEL spectrum, the leak valve was closed and the chamber evacuated again to the low 10^{-10} mbar range, before transferring the sample back to the analysis chamber.

III. THEORETICAL APPROACH

Calculations of the GaAs(001) surface were performed using density functional theory in the local density approximation (DFT-LDA). Besides the well-known $\beta 2$ model of the (2×4) phase, we considered the mixed dimer model for the $c(4\times4)$ reconstruction. As suggested by several recent works,[11,16–18] a mixed dimer structure—as distinct from the more traditional symmetric dimer model—should be formed if the above experimental preparation conditions are adopted. Both structures are shown schematically in Fig. 1. The systems were modeled using periodically repeating supercells of thin GaAs slabs, 10 layers $[\beta 2(2\times4)]$ and 11 layers $[c(4\times4)]$ thick, respectively, separated by about 10 Å of vacuum in each case. Computation was carried out using the ABINIT code[19] and a local Car-Parrinello code, within a framework of planewaves (of kinetic energy cut-off 18 Ry) and norm-conserving pseudopotentials (of the Hamann type) to obtain the relaxed surface geometry and wave functions. Nonlinear core corrections[20] were used for gallium. During structure optimization the back two layers were fixed at the bulk positions; furthermore, the back surface was terminated with fractionally charged hydrogens. Optimization was performed until forces were converged to 35 meV/Å. The theoretical value for the lattice constant, $a_0=5.58$ Å, was used. Relativistic effects are not included. These settings, as well as the use of a single **k** point during the geometry optimization, were previously found to yield structural parameters in excellent agreement with other calculations.[17]

The energy loss function was calculated using the anisotropic three-layer model of Del Sole and Selloni,[21] in which the surface is represented by a layer of thickness d and as having dielectric tensor ε_s. Further detailed expressions for the calculated HREELS quantities have been presented in previous articles[8,9] For both (2×4) and $c(4\times4)$ structures, ε_s was calculated at the RPA level using 18 **k** points in the irreducible part (one quarter) of the surface Brillouin Zone. This **k**-point set yielded spectral features converged to a precision in energy of about 0.1 eV. In order to account for self-energy and excitonic shifts in energy (and also, to some extent, finite temperature effects), we apply a rigid scissors shift Δ to the unoccupied states, according to the scheme of Del Sole and Girlanda.[22] The value of Δ also depends to some extent on finite temperature effects and on the influence of size quantization due to the finite slab approximation. By adopting $\Delta=0.3$ eV and $\Delta=0.5$ eV for the (2×4) and $c(4\times4)$ surfaces, respectively, we obtain the best agreement with experiment in each case. For comparison, we note that the self-energy shift in the *bulk* (not accounting for excitonic effects) is about 0.8 eV[23]. The same shift was used by some of us in calculations of the RAS of the $c(4\times4)$ surface.[17] The need for two different shifts is a consequence of the different electronic structures in the two surface reconstructions. In general, surface states and extended states (such as surface-perturbed bulk states) are affected differently by size quantization; they also require different self-energy corrections (see, e.g., Ref. 23). In the present case, transitions involving extended states dominate the (2×4) surface spectra,[4,25] while transitions below 3.0 eV in the $c(4\times4)$ are strongly localized within the topmost layers.[17] Excitonic effects may also differ for each reconstruction. The appearance of different shifts was effectively demonstrated by Schmidt and co-workers (Ref. 25), who calculated self-energy corrections in the range of 0.6–0.9 eV in both systems. Only in the case of the (2×4) surface, however, was this correction found to be too large (by 0.3–0.4 eV) with regard to experiment.

IV. $\beta 2(2\times4)$ PHASE: RESULTS AND DISCUSSION

A. Experimental results

The HREEL spectra measured along $[1\bar{1}0]$ and [110] are presented in Fig. 2, for the clean surface and for oxygen exposures ranging from 50 L to 5 KL. In the [110] direction the loss intensity rises sharply at the energy gap value of 1.5 eV, features a shoulder at 1.7 eV and a maximum at 2.6 eV, and then declines slightly, before increasing again at

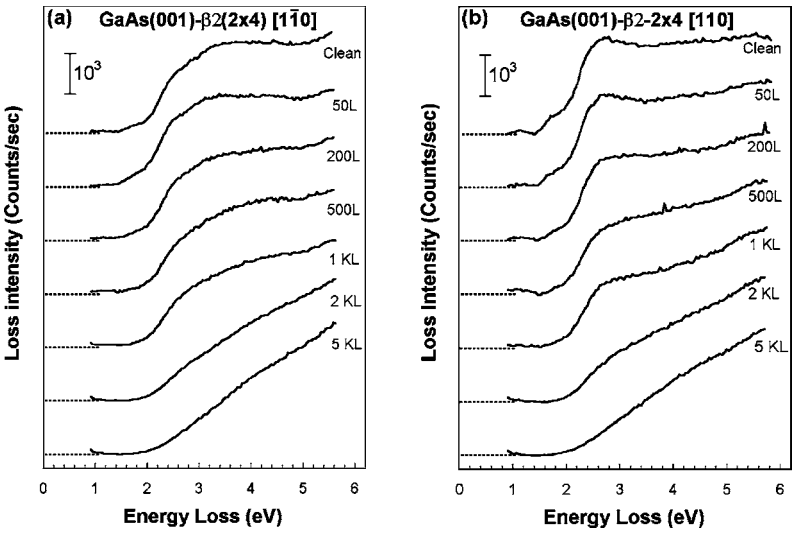

FIG. 2. HREEL spectra acquired on the $\beta 2(2\times 4)$ surface along the (a) $[1\bar{1}0]$ and (b) $[110]$ directions, for successive oxygen exposures up to 10 KL.

higher energies. In the $[1\bar{1}0]$ direction a smoothly increasing spectrum is measured with an additional broad peak at around 3.5 eV.

The structures in both directions are observed to progressively vanish for increasing coverages of oxygen, until the curves become equal at an oxygen exposure of about 5 KL, where they show only a very faint structure centered around 4 eV. A detailed analysis of structure decays reveals that the spectra, in both directions, are characterized by three main features: A shoulder at 1.8 eV, the main peak around 2.6 eV, and a weak structure, only visible along the $[1\bar{1}0]$ azimuth, at about 3.5 eV. Each structure was analyzed by means of a background subtraction and a Gaussian fit. Several backgrounds[24] were employed and were found to yield similar results with the subsequent Gaussian fit.

It is worth pointing out that there is a remarkable similarity between the spectra of the decapped surface, shown in a previous work,[8] and the spectra of the *as-grown* surface exposed to 200–500 L of oxygen (Fig. 2): Features above the gap are broadened and the spectra themselves are vertically offset by a broad background signal. This observation provides by itself a sensitive method to test the surface quality after the As decapping procedure. We stress that the strong surface reactivity to oxygen observed here is peculiar to loss spectroscopy and has no counterpart, for this surface, in the oxidized RAS spectra, especially in the energy region above 2.6–2.7 eV.[9] In fact, RAS spectra present a huge peak at 2.9 eV (related to bulk states modified by the surface) overlapped with a negative and broad surface structure between 1.6 and 2.6 eV,[9,25] detectable when the surface quality is very high.[9] The sensitivity of the former feature to oxygen is well below that observed for the pure surface states measured by HREELS.

The peak intensity behavior versus the oxygen exposure along the two azimuthal directions follows a simple exponential decay law:

$$I(x) = I_0 e^{-x/x_d}, \tag{1}$$

where x is the oxygen exposure and x_d the oxidation decay constant. The decay rates of the structures are reported in Table I. For the 2.6 eV (both directions) and 3.5 eV structures the rates are practically the same: x_d ranges between 1.4 and 1.7 KL. A faster decay is apparent for the structure at 1.8 eV, indicating that the electronic states responsible for this peak are directly involved, if not completely quenched, in the initial stages of oxygen adsorption. We now identify these states by means of microscopic calculations of the surface electron energy loss spectra.

B. Analysis of clean surface spectra

Theoretical results for the HREELS spectra of clean GaAs(001)-$\beta 2(2\times 4)$ are presented in Fig. 3 and compared with the experimental data. To obtain the true experimental surface spectra, we have subtracted, in Fig. 2(a), a suitable background signal[26] from the measured signals of Fig. 2 for both $[1\bar{1}0]$ and $[110]$ directions. The resulting spectra compare reasonably well with the calculated spectra shown in Fig. 3(b). However, a better comparison is the relative difference spectra, as shown in Fig. 3(c), for which many unknown quantities, such as those related to the background, cancel out. Good agreement is found up to about 3.5 eV, although the theoretical intensity is somewhat underestimated. The experimental features in the bare EELS curves occurring at 1.8 eV (S_1), 2.6 eV (S_2), and 3.5 eV (S_3) translate to more well defined structures in the difference spectrum at 1.8–2.0 eV, 2.4–2.7 eV, and 3.4–3.7 eV. These structures correspond to peaks in the calculation at 2.0 and 2.6 eV, and to the broad structure at 3.1–3.5 eV [Fig. 2(c)]. The small negative structure appearing in the calculation at

TABLE I. Decay constants for the $\beta 2(2\times 4)$ surface.

	Peak position (eV)	Azimuth	$x_d(KL)$
S_1	1.8	$[110]$	0.61 ± 0.05
S_2	2.6	$[110]$	1.39 ± 0.17
	2.6	$[1\bar{1}0]$	1.49 ± 0.16
S_3	3.5	$[1\bar{1}0]$	1.61 ± 0.13

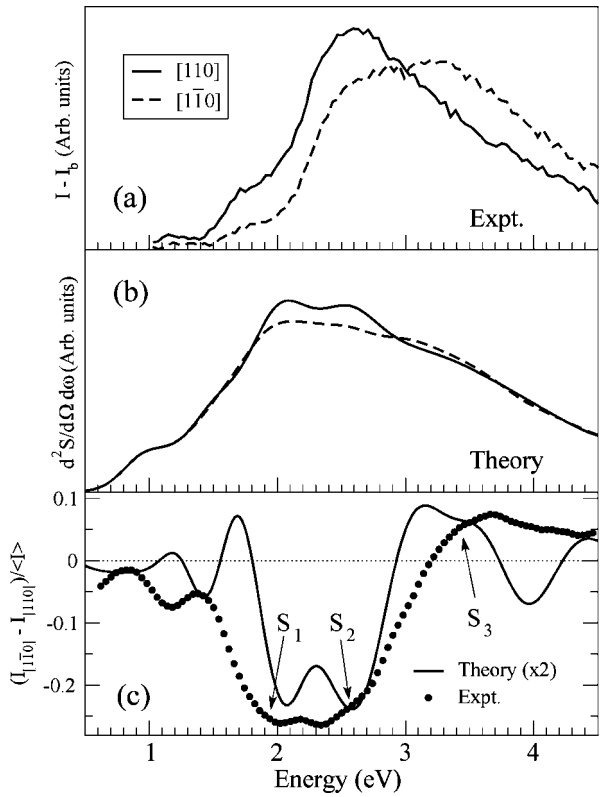

FIG. 3. Experimental and calculated HREELS spectra for the clean $\beta 2(2\times4)$ reconstruction. Top: Experimental spectra for q oriented along the $[1\bar{1}0]$ and [110] directions after subtraction of background. Center: Calculated spectra for $[1\bar{1}0]$ and [110] directions. Bottom: Relative difference spectra. All theoretical spectra are shown for Gaussian broadenings of FWHM 0.4 eV.

1.4 eV may correspond to that at 1.2 eV in the experiment, but since it was found to derive from a single transition within this **k**-point set, it might be spurious.

We determined the microscopic origins of the energy loss spectrum by coupling an analysis of the electronic states associated to each peak with a real-space decomposition of the surface dielectric function (similar to that reported for RAS in Ref. 10). This procedure enables us to extract precise spatial information about the origin of spectral features. Characteristic states associated with the three main features are shown in Fig. 4 as contour maps of the squared wave function. The S_1 peak [Fig. 4(a)] is found to derive from transitions occurring along the $\Gamma-J'$ direction within the region bounded by the second and fourth atomic layers: Initial states are surface resonances or surface-perturbed bulk states {V1} with a significant localization at the third layer As atoms (including, in particular, the *dimer* atoms); final states are associated with antibonding orbitals of the third layer dimer {C1}, the p_z-like orbitals of the second layer Ga (not apparent for the state shown here), and other third layer As atoms.

The S_2 peak [Fig. 4(b)], on the other hand, is known[4] to be strongly localized within the topmost layers and to arise from transitions between occupied dimer backbond states {V2} and the unfilled Ga dangling bonds {C2}, yielding a dominant signal along the [110] direction. The third resolved feature, S_3, arises instead from subsurface layers and has less

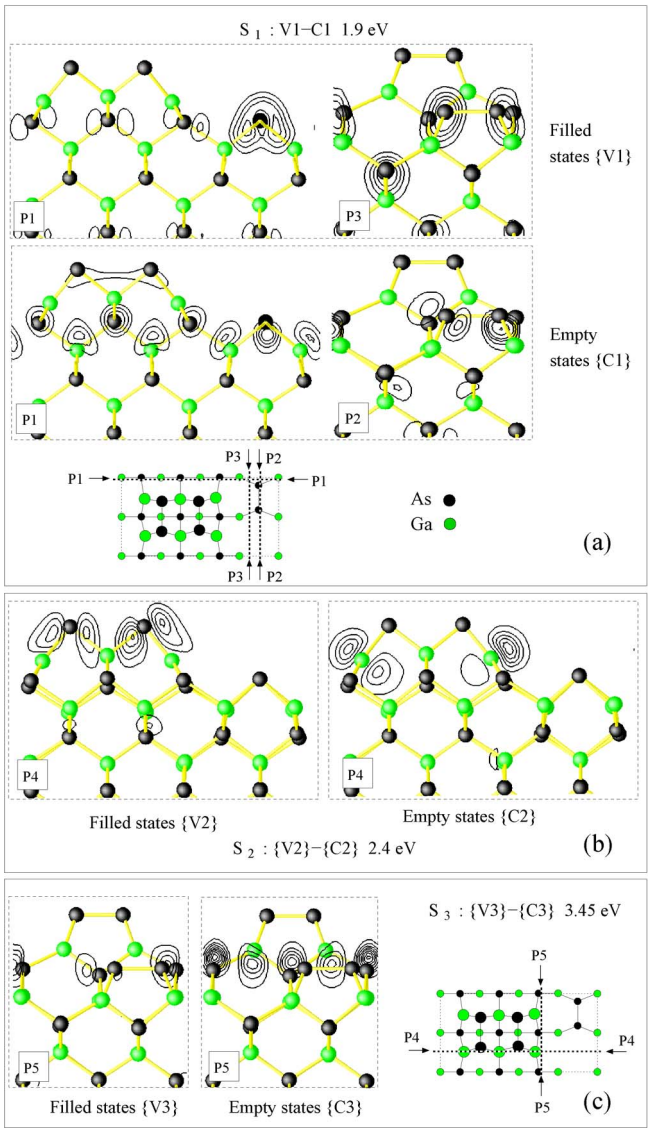

FIG. 4. (Color online) Contour plots of characteristic states (wave function squared) contributing to the S1, S2, and S3 peaks in the energy loss spectrum of GaAs(001)-$\beta 2(2\times4)$. Contours are mapped onto the planes Pn as indicated in the schematic diagrams. As a guide to the eye, the contours are superimposed on a perspective view of the atomic structure.

clearly defined origins: Unoccupied states are generally aligned along $[1\bar{1}0]$ and are delocalized throughout the slab [an example is {C3}, shown in Fig. 4(c)], whereas occupied states {V3} are surface-perturbed bulk states or resonances involving the top or third layer As atoms (typically not the third layer dimer, however).

C. Discussion

In the previous section we demonstrated how theoretical calculations of the energy loss spectra of the *clean* GaAs(001)-$\beta 2(2\times4)$ surface are able to explain the microscopic origins of the corresponding experimental spectra. A thorough understanding of the *oxidized* spectra would re-

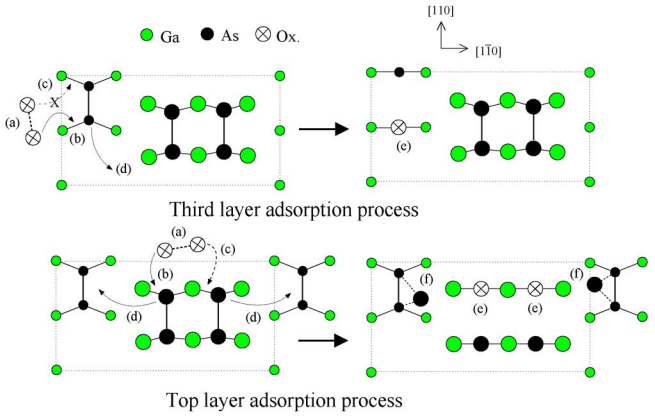

FIG. 5. (Color online) Schematic representation of two possible dissociative chemisorption processes at the $\beta 2(2\times4)$ surface. In (a), the oxygen molecule approaches a region of high electronic charge, i.e., the As dimer(s) in the top or third layer. Dissociation of O_2 occurs when one O atom attacks a As–Ga backbond (b), and displaces an As atom (d). The remaining O atom may substitute an adjacent As atom (c), although this is not favored for both As atoms in a dimer. Oxygen remains bound to the surface in Ga–O–Ga bonds (e). As atoms displaced from the topmost dimers cluster at the third-layer dimer site (f). Only the "top layer absorption process" has actually been observed (see text).

quire, however, calculation of the structure and optical properties for various oxidized configurations and coverages, which is beyond the scope of the present work. Nevertheless, it is useful to see whether the present analysis can add to (or can at least be consistent with) our understanding of the oxidation mechanisms.

Previously, it has been shown from STM measurements[13,27] and DFT-LDA cluster calculations[13,27] that the molecular phase of oxygen dissociatively chemisorbs to the GaAs(001)-$\beta 2(2\times4)$ surface. Substitution of top-layer As dimer atoms, with subsequent dimer breaking and formation of Ga–O–Ga bonds, is found to be the dominant process.[12,28] An important side effect, as observed in the STM images,[12,13] is the clustering of displaced As atoms at the third layer dimer region. The various stages in the oxidation process are outlined schematically in Fig. 5, for absorption at the top layers (as observed) and at the third layer (as a second possibility).

Since the S_1 structure decays fastest, it is reasonable to deduce from our theoretical analysis of the peaks that initial oxygen adsorption occurs at the third layer dimer region. Breaking of these dimers would directly quench S_1, as it involves dimer-localized states ({V1} in Fig. 4, for instance); in contrast, the states contributing to S_2 are backbond-or Ga-localized, and may not be destroyed as effectively following dimer breaking. Although molecular oxygen adsorption in the dimer trough region has not been observed, we note that resolution of the scanning tunneling microscopy (STM) to the third layer is extremely difficult, and is achievable only within specific conditions.[29] On the other hand, adsorption at the third layer dimer is less thermodynamically favorable than at the top layer, where O–Ga–O bond formation is possible (see Fig. 5, bottom-right panel). Furthermore, the highly electrophilic oxygen should be attracted initially towards the larger concentration of electronic charge occurring at the top dimer region. Steric effects and the relative lack of adsorption sites may also slow adsorption at the third-layer dimer.

An alternative suggestion, which accounts for all given data in a more consistent manner, is the following: The rapid decay of S_1 is caused by, or at least enhanced by, clustering of displaced As in the trough. This is most strongly evidentiated by the fact that this clustering has been experimentally observed,[12,13] and hence must influence the EELS spectra. In fact, if we assume that all displaced As atoms move to the third layer region and perturb the dimer states, the decay rate of S_1 could be twice that of S_2 (in fact, it is higher: see Table I). The S_2 (and S_3) feature, on the other hand, gradually decays with oxygen exposure as all top-layer dimers are broken, Ga–O–Ga bonds are formed and overall disorder increases. Finally, S_3 likely decays slowest as its states are the least strongly localized at the surface, and generally unassociated with the dimers.

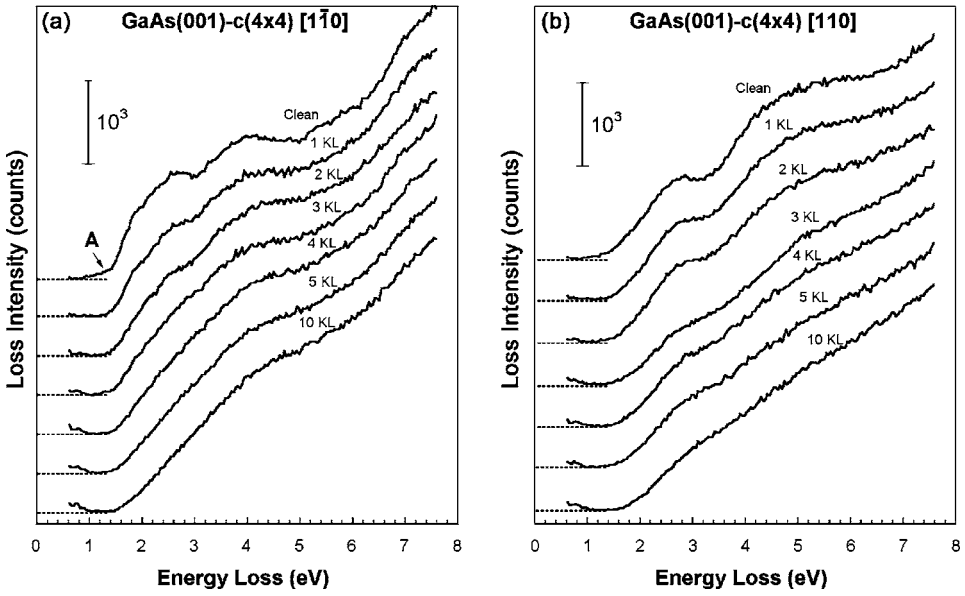

FIG. 6. HREEL spectra acquired on $c(4\times4)$ surface along [1$\bar{1}$0] (a) and [110] direction (b), for successive oxygen exposure up to 5 KL.

TABLE II. Decay constants for the c(4×4)) surface.

	Peak position (eV)	Azimuth	$x_d(KL)$
S_1	1.8	$[1\bar{1}0]$	2.9±0.3
S_2	2.25	$[1\bar{1}0]$	4.3±0.8
S_3	2.7	[110]	5.0±1.2

V. $c(4\times4)$ PHASE: RESULTS AND DISCUSSION

A. Experimental results

HREEL spectra for the $c(4\times4)$ surface are shown in Fig. 6 for the $[1\bar{1}0]$ and [110] directions, and are seen to exhibit several distinct features. For the clean surface, along $[1\bar{1}0]$, a doublet is observed between 1.8 and 2.25 eV, with a bump centered at 4 eV. In contrast, along [110], the spectrum displays an asymmetric structure centered at 2.7 eV and a huge and broad peak around 5 eV. Notably, the leading edges of the two spectra are quite different: In the [110] direction the loss intensity starts sharply around 1.5 eV, the $[1\bar{1}0]$ spectrum exhibits a gradual increase from 1.0 eV followed by a steeper increase at 1.5 eV, similar to the surface but not as significant. This anisotropic response mirrors that of the $\beta2(2\times4)$ surface (Fig. 2) where the [110] spectrum, with $\mathbf{q}_\parallel$ perpendicular to dimers in this case, is more structured than the $[1\bar{1}0]$ spectrum.

Features in both directions are observed to progressively vanish for increasing coverages of oxygen, just as in the case of the $\beta2(2\times4)$. Several remarks reported in Ref. 7 are confirmed. One notable feature of Fig. 6(a) is the little shoulder, labeled A in Fig. 6, appearing at 1.2 eV, above the level of noise in the spectrum, along the [110] direction, which disappears permanently after the first exposure to 1 KL of oxygen. This confirms that its nature is strictly related to localized surface states or to defects. On the other hand, all other structures generally decrease until complete disappearance occurs at about 4 KL along both directions.

As before, each peak presents a simple exponential decay law with respect to oxygen exposure with the form of Eq. (1). The highest sensitivity to oxidation has been found for the structure at 1.8 eV detected along the $[1\bar{1}0]$ azimuth, while the decay of peaks centered at 2.25 eV (along the $[1\bar{1}0]$) and 2.7 eV (along the [110]) respectively, show similar behavior. In Table II the exponential decay constant x_d for each peak is reported. The error takes into account the errors on the best fit performed after the background subtraction. As may be noted, the oxygen exposure necessary for a peak to decrease by a factor e^{-1} ranges between 3 and 5 KL as well has been observed for RAS structures.[9]

B. Analysis of clean surface spectra

In Fig. 7(a) we show the HREEL spectra of the clean GaAs(001)-$c(4\times4)$ surface acquired along $[1\bar{1}0]$ and [110], after subtraction of a typical background signal. As noted for the $\beta2(2\times4)$ surface, the oxygen-sensitive features deduced

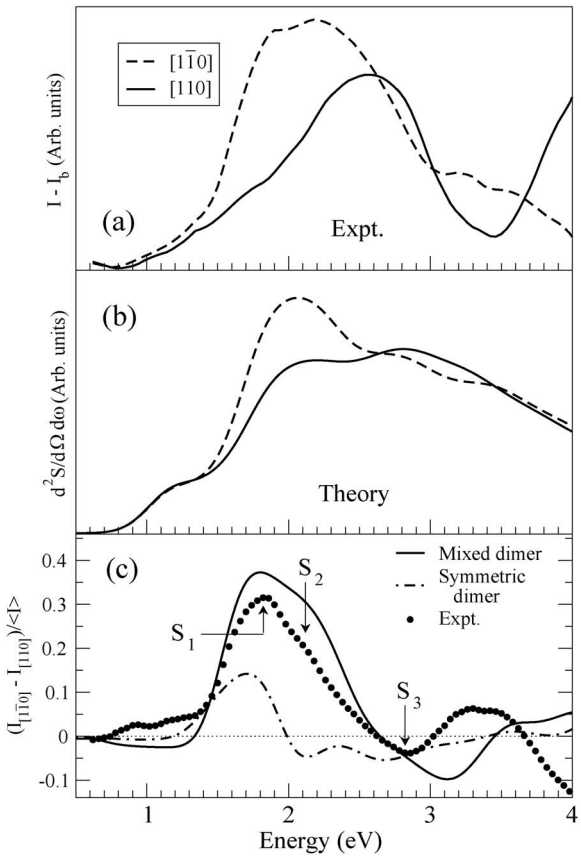

FIG. 7. Experimental and calculated HREELS spectra for the clean $c(4\times4)$ reconstruction. Top: Experimental spectra for q oriented along the $[1\bar{1}0]$ and [110] directions after subtraction of background. Center: Calculated spectra for $[1\bar{1}0]$ and [110] directions. Bottom: Relative difference spectra, normalized to the experimental intensity. Theoretical spectra have a Gaussian broadening of FWHM=0.4 eV.

from the HREEL spectra of Fig. 6 are clearly related to structures in the relative difference spectra [Fig. 7(c)]: A sharp positive peak at 1.8 eV (S_1) with a shoulder at about 2.2 eV (S_2), and a small negative peak at 2.7 eV (S_3). It is notable that the S_1 peak is comparable in intensity—albeit opposite in sign—to the S_1 structure, also occurring around 1.8 eV, of the $\beta2$ surface (see Fig. 3). This is consistent with the opposite direction of the dimers in each case, with transitions occurring along the direction of the dimer *rows* in each case. Indeed, HREEL spectra below about 3 eV generally show structures associated with the presence of the missing dimer row, as we showed for the $\beta2(2\times4)$ surface (Sec. IV B), and will also now show for the $c(4\times4)$ surface.

Although the bare spectra are qualitatively comparable with the results of the theoretical calculations [Fig. 7(b)] up to about 3 eV, a more realistic comparison with experiment is obtained for the relative difference spectra, shown in Fig. 7(c) (solid and dotted lines). Both S_1 and S_2 peaks are recovered by the theory, although the final feature at 2.7 eV (S_3) is blue shifted to 3.1 eV. This discrepancy is largely due to the limitations of the current theoretical scheme, which in fact fails completely to describe the experimental data above

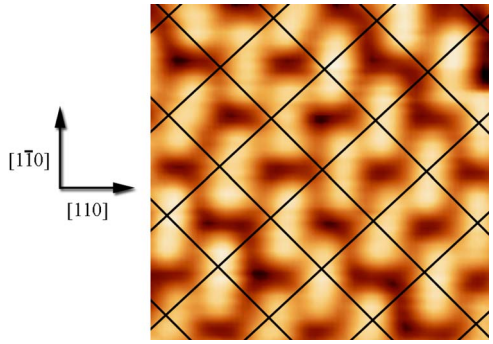

FIG. 8. (Color online) Empty-state STM image (5.3×5.3 nm^2 of the $c(4\times4)$ surface acquired at 80 K using a bias of 4 eV. The solid lines show the $c(4\times4)$ lattice mesh.

3.5 eV.[30] Nevertheless, this does not influence our analysis of the spectral peaks, since the important quantity for analysis—the imaginary part of the surface dielectric anisotropy—features peaks near the correct energies (1.8, 2.0, and 2.5–2.7 eV). We note that the spectra in Fig. 7(b) are not peaked at 1.2 eV, as found in earlier calculations.[7] This is possibly due to the smaller slab thickness (7 layers) adopted in that work. Earlier calculations by some of us,[7] in which the symmetric dimer reconstruction was assumed, also found good agreement with experiment (a larger shift of 0.62 eV was also used). However, we have confirmed that the slab thickness (7 layers) adopted in that work is insufficient to yield well converged atomic positions in the topmost layers. Therefore, we regard the calculated geometry of that work as being not enough accurate so as the resulting HREELS spectra (for the same reason, we must regard the peak found at 1.2 eV in that work to be spurious).

Finally, we draw attention to the dash-dotted line in Fig. 7(c), which is the relative difference spectrum calculated for a $c(4\times4)$ reconstruction terminated by three As–As dimers. The spectrum is in poor agreement with experiment, particularly as the S_2 peak is of the wrong sign. As the STM image of our $c(4\times4)$ surface already indicates a mixed dimer structure (see Fig. 8), the HREELS results provides further evidence that this structure is formed under the experimental conditions outlined in Sec. II. Such findings are in full agreement with recent papers.[11,16,17]

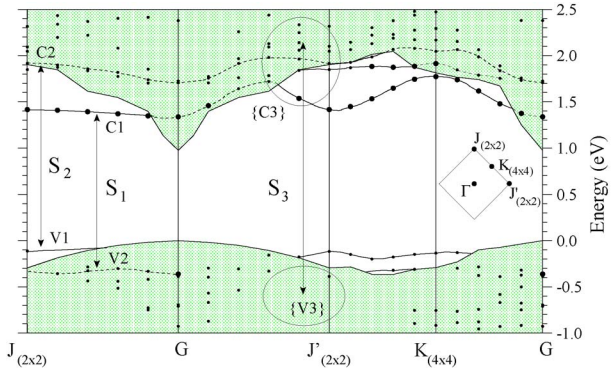

FIG. 9. (Color online) Band structure of the $c(4\times4)$ surface, with main optical transitions marked. A rigid shift of +0.5 eV has been applied to the conduction bands.

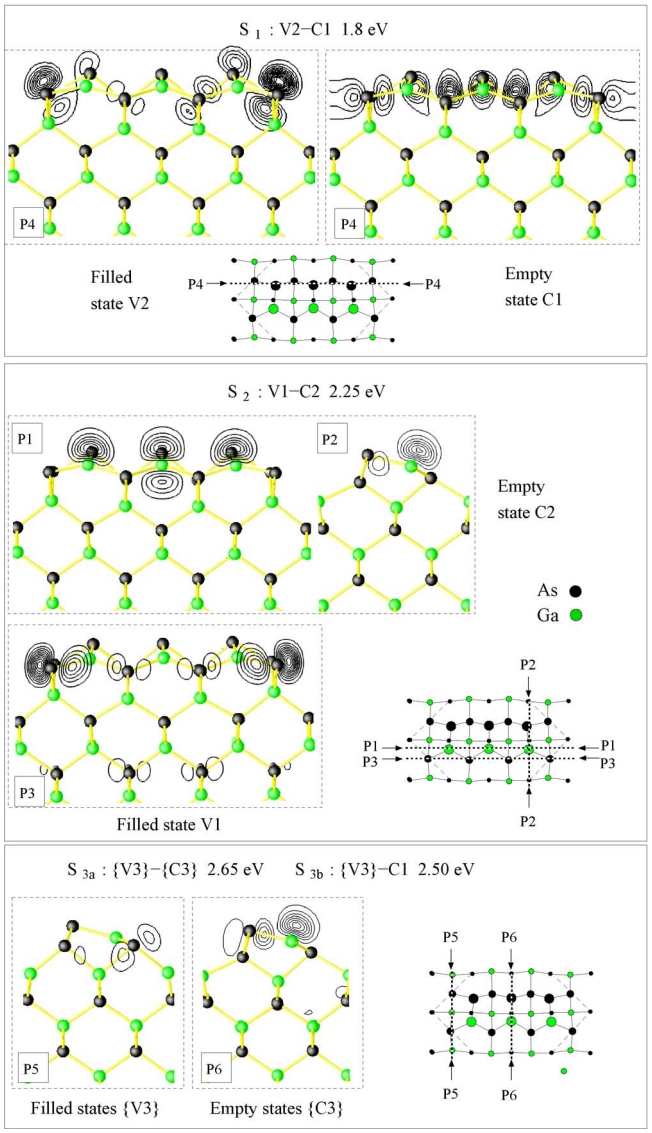

FIG. 10. (Color online) Contour plots of states (wave function squared) giving rise to the S_1, S_2, and S_3 peaks in the energy loss spectrum. Contours are mapped onto the planes Pn as indicated in the schematic diagrams, and superimposed on a perspective view of the atomic structure as a guide to the eye.

We now analyze the spatial and electronic origins of the HREEL spectra in the same manner as was done for the $\beta2(2\times4)$ surface spectra. Hence, real-space maps of the relevant states (wave function squared) are shown in Fig. 10 for each the three major peaks. Since the states involved in the S_1 and S_2 peaks are found to be strongly localized within the top 2 to 3 atomic layers, it is possible to directly visualize the transitions within the surface band structure, which is reported in Fig. 9. Note the relevance in Fig. 10 of the four threefold-coordinated As atoms that are situated in the second layer at the ends of the three-dimer block. In particular, the $V1$ and $V2$ bands appear to be associated with filled dangling-bond orbitals at these sites.

Regarding the three HREELS features, the S_1 peak derives from transitions between p_z-like states ($V2$) localized on the two such As atoms situated on the As-rich side of the

dimer block [i.e., cutting plane P4 in Fig. 10(a)] and the conduction band state $C1$, which is highly localized within the chain of surface As atoms directed along $[1\bar{1}0]$. Similarly, S_2 involves transitions from $V1$, a p_x-like state located on the other two such second layer As atoms (i.e., those bonded to the Ga dimer atoms); unoccupied states are p_z-like states corresponding to the top layer Ga dangling bonds ($C2$). Both S_1 and S_2 occur along the $\Gamma-J$ direction in **k**-space. The S_3 peak, on the other hand, is derived from transitions along $\Gamma-J'$ between various surface-perturbed bulk states $\{V3\}$ (weakly localized on the aforementioned second-layer As atoms) and dimer localized surface resonances $\{C3\}$—again, with a strong p_z-like shape on the sp^2 coordinated Ga atoms—or, to a lesser extent, from the $\{V3\}$ states to the $C1$ states. Note that none of the relevant states is directly associated with dimer "bonding" orbitals.

C. Discussion

The mechanisms of oxygen adsorption at the $c(4\times4)$ surface appear to be quite different from those at the $\beta2(2\times4)$ judging by the difference in decay constants (up to a factor of five for S_1). After an exposure of 5 KL the $\beta2(2\times4)$ loss spectra are practically smooth (Fig. 2); on the contrary, in the $c(4\times4)$, some structural traces are still detectable after 10 KL. This indicates that the As-rich double layer appearing on top of the $c(4\times4)$ surface acts as a stable "cap," rendering it less reactive.

The effectiveness of this cap is particularly interesting when the EELS spectra are considered, since the S1, S2, and S3 transitions are characterized by transitions very strongly localized within the topmost layers. Even the optically active As sites on the (exposed) second layer (important for V1 and V2) appear to be relatively unaffected by oxygen. The rates of decay for the three structures are quite similar, suggesting that a single adsorption site does not dominate. An important point is that Ga–O–Ga bonds, which were noted in Sec. IV C to be highly favoured during the oxidation of the $\beta2(2\times4)$ surface, are not easily formed at this surface. Unfortunately, no STM (or other) studies exist to our knowledge for the oxidized surface which might help us interpret the EELS spectra. We were unable to form a precise description of the oxidation mechanism, due to the large range of possible structures and precursors, ranging from molecular chemisorption[31] to the presence of nonbridging As=O double bonds[32] or bridging As–O–Ga bonds,[33,34] as have been suggested for oxidized GaAs(110) surfaces. Further theoretical modeling in this direction would be instructive.

VI. CONCLUSIONS

HREELS measurements performed on GaAs(001) surfaces exposed to molecular oxygen highlight the higher sensitivity of $\beta2(2\times4)$ to oxygen in comparison with $c(4\times4)$. These findings, together with the results in Ref. 12, allow us to attribute a general higher reactivity of molecular oxygen with As–Ga bonds in comparison with As–As bonds.

The oxidation kinetics of both HREELS and RAS for the $c(4\times4)$ surface[8,9] are similar, indicating a common microscopic origin. Conversely, for the $\beta2(2\times4)$ surface, the decay rate of the HREELS structures is faster than that of the RAS structures: This is wholly in agreement with theoretical calculations which assign, for the most part, a bulk origin to the RAS signal.[25,35]

ACKNOWLEDGMENTS

The authors thanks F. Ronci, S. Colonna, and A. Cricenti for the STM measurements on $c(4\times4)$ surface. C.H. and R.D.S. acknowledge financial support from the NANOQUANTA Network of Excellence (Contract No. NMP4-CT-2004-500198), and super-computing time at CINECA under Grant No. cmprmpi9.

*Electronic address: placidi@roma2.infn.it

[1] S. Selci, F. Ciccacci, G. Chiarotti, P. Chiaradia, and C. Cricenti, Surf. Sci. **5**, 327 (1987).
[2] P. Chiaradia and G. Chiarotti, in *Photonic Probes of Surfaces*, edited by P. Halevi (Elsevier Science, Amsterdam, 1995), Vol. 2, p. 99.
[3] V. L. Berkovits, P. Chiaradia, D. Paget, A. B. Gordeeva, and C. Goletti, Surf. Sci. **441**, 26 (1999).
[4] D. Paget, C. Hogan, V. L. Berkovits, and O. E. Tereshchenko, Phys. Rev. B **67**, 245313 (2003).
[5] D. Pahlke, M. Arens, N. Esser, D. T. Wang, and W. Richter, Surf. Sci. **352**, 66 (1996).
[6] M. Arens, M. Kuball, N. Esser, W. Richter, M. Cardona, and B. O. Fimland, Phys. Rev. B **51**, 10923 (1995).
[7] A. Balzarotti, F. Arciprete, M. Fanfoni, F. Patella, E. Placidi, G. Onida, and R. Del Sole, Surf. Sci. Lett. **524**, 71 (2003).
[8] A. Balzarotti, E. Placidi, F. Arciprete, M. Fanfoni, and F. Patella, Phys. Rev. B **67**, 115332 (2003).
[9] F. Arciprete, C. Goletti, E. Placidi, P. Chiaradia, M. Fanfoni, F. Patella, C. Hogan, and A. Balzarotti, Phys. Rev. B **68**, 125328 (2003).
[10] F. Arciprete, C. Goletti, E. Placidi, C. Hogan, P. Chiaradia, M. Fanfoni, F. Patella, and A. Balzarotti, Phys. Rev. B **69**, 081308(R) (2004).
[11] A. Ohtake, P. Kocán, J. Nakamura, A. Natori, and N. Koguchi, Phys. Rev. Lett. **92**, 236105 (2004).
[12] P. Kruse, J. G. McLean, and A. C. Kummel, J. Chem. Phys. **113**, 9224 (2000).
[13] S. I. Yi, P. Kruse, M. Hale, and A. C. Kummel, J. Chem. Phys. **114**, 3215 (2001).
[14] F. Fuchs, W. G. Schmidt, and F. Bechstedt, Phys. Rev. B **72**, 075353 (2005).
[15] A. Incze, R. Del Sole, and G. Onida, Phys. Rev. B **71**, 035350 (2005).
[16] A. Ohtake, J. Nakamura, S. Tsukamoto, N. Koguchi, and A. Natori, Phys. Rev. Lett. **89**, 206102 (2002).

[17] C. Hogan, E. Placidi, and R. Del Sole, Phys. Rev. B **71**, 041308 (2005).
[18] M. Takahasi and J. Mizuki, Phys. Rev. Lett. **96**, 055506 (2006).
[19] The ABINIT code is a common project of the Université Catholique de Louvain, Corning Incorporated, and other contributors (http://www.abinit.org).
[20] S. G. Louie, S. Froyen, and M. L. Cohen, Phys. Rev. B **26**, 1738 (1982).
[21] A. Selloni and R. Del Sole, Surf. Sci. **186**, 35 (1986).
[22] R. Del Sole and R. Girlanda, Phys. Rev. B **48**, 11789 (1993).
[23] O. Pulci, G. Onida, R. Del Sole, and L. Reining, Phys. Rev. Lett. **81**, 5374 (1998).
[24] We tried various forms of background signal, e.g., linear, quasi-linear, and Shirley as well as the HREELS spectrum for the fully oxidized surface.
[25] W. G. Schmidt, F. Bechstedt, K. Fleischer, C. Cobet, N. Esser, W. Richter, J. Bernholc, and G. Onida, Phys. Status Solidi A **188**, 1401 (2001).
[26] The background used is the EELS spectrum measured after the final oxidation.
[27] M. Hale, S. I. Yi, J. Z. Sexton, A. C. Kummel, and M. Passlack, J. Chem. Phys. **119**, 6719 (2003).
[28] J. Z. Sexton, S. I. Yi, M. Hale, P. Kruse, A. A. Demkov, and A. C. Kummel, J. Chem. Phys. **119**, 9191 (2003).
[29] V. P. LaBella, H. Yang, D. W. Bullock, and P. M. Thibado, Phys. Rev. Lett. **83**, 2989 (1999).
[30] A model of energy loss which includes the q dependence and avoids the three-layer approximation also fails to reproduce the broad feature at 5 eV, although the correct energy position of the S_3 peak is recovered [C. Hogan, R. Del Sole, and A. Marini (unpublished)].
[31] V. L. Berkovits, N. Witkowski, Y. Borensztein, and D. Paget, Phys. Rev. B **63**, 121314(R) (2001).
[32] D. H. Lee, J. Chung, and S.-J. Oh, Phys. Rev. B **53**, 13038 (1996), and articles referred to therein.
[33] C. Y. Su, I. Lindau, P. W. Chye, P. R. Skeath, and W. E. Spicer, Phys. Rev. B **25**, 4045 (1982).
[34] K. A. Bertness, J.-J. Yeh, D. J. Friedman, P. H. Mahowald, A. K. Wahi, T. Kendelewicz, I. Lindau, and W. E. Spicer, Phys. Rev. B **38**, 5406 (1988).
[35] W. G. Schmidt, F. Bechstedt, W. Lu, and J. Bernholc, Phys. Rev. B **66**, 085334 (2002).